*Article*

# Highway Ecological Environmental Assessment Based on Modified Remote Sensing Index—Taking the Lhasa–Nyingchi Motorway as an Example

Xinghan Wang [1,2,†], Qi Liu [2,†], Pengfei Jia [3,*], Xifeng Huang [4], Jianhua Yang [5], Zhengjun Mao [6] and Shengyu Shen [7,8]

1    College of Civil Engineering, Tianjin University, Tianjin 300350, China; wxhan@tju.edu.cn
2    Research Center on Flood & Drought Disaster Reduction of the Ministry of Water Resources, China Institute of Water Resources and Hydropower Research, Beijing 100038, China; liuqi@iwhr.com
3    Citic Construction Co., Ltd., Beijing 100027, China
4    Shaanxi Provincial Water Resources Department, Xi'an 710004, China; hxf_sxsl@163.com
5    Academy of Eco-Civilization Development for Jing-Jin-Ji Megalopolis, Tianjin Normal University, Tianjin 300387, China; yangjh15@mail.bnu.edu.cn
6    College of Geology and Environment, Xi'an University of Science and Technology, Xi'an 710054, China; mzj@xust.edu.cn
7    Department of Soil and Water Conservation, Changjiang River Scientific Research Institute (CRSRI), Wuhan 430010, China; shenshengyu@mail.crsri.cn
8    Research Center on Mountain Torrent & Geologic Disaster Prevention of the Ministry of Water Resources, Wuhan 430010, China
*    Correspondence: jiapf@citic.com
†    Co-first author: Qi Liu.

**Abstract:** The Lhasa to Nyingchi Expressway in Xizang made efforts to protect the ecological environment during its construction, but it still caused varying degrees of damage to the fragile ecosystems along the route. Accurately assessing the process of change in the ecological environment quality in this region holds significant research value. This study selected the Linzhi-to-Gongbo'gyamda section of the Lhasa-to-Nyingchi Expressway as the research area. Firstly, based on the remote sensing ecological index (RSEI), this study constructed an ecological environmental quality evaluation system for the Xizang region. Subsequently, using the Google Earth Engine (GEE) platform, sub-indicators were extracted, and the combination weighting method of game theory was employed to determine indicator weights. This process resulted in the calculation of the MRSEI for the study area from 2012 to 2020. Finally, by utilizing the spatial distribution of the MRSEI, monitoring the level of MRSEI changes, and employing the transition matrix, this study analyzed the changing trend of the ecological environmental quality from 2012 to 2020. The results indicate that the MRSEI are 0.5885, 0.5951, 0.5296, 0.6202, 0.59, 0.5777, 0.5898, 0.5703, and 0.5987, showing a gradual increasing trend with an initial decrease followed by an ascent. This trend is mainly attributed to concentrated road construction and subsequent ecological restoration, leading to an improvement in the restoration effect. Simultaneously, the ecological environmental quality remains relatively stable, with 69.5% of the region showing no change, and the remaining 30.5% experiencing improvement exceeding degradation. Specifically, there were significant improvements in the land with ecological quality levels categorized as poor, fair, moderate, and good. The types of degradation primarily involved lands originally classified as excellent and good degrading to good and moderate levels, respectively. The above results serve as a theoretical reference for the ecological restoration project of the Lhasa-to-Nyingchi Expressway.

**Keywords:** GEE; RSEI; ecological environmental quality; Lhasa–Nyingchi Motorway

## 1. Introduction

The Xizang region is an important ecological security zone in China, with natural protected areas accounting for one-third of the total area. The Lhasa–Nyingchi Motorway in the Xizang region not only benefits local economic development and the development and utilization of natural resources but also contributes to border stability and the common prosperity of all ethnic groups. However, on one hand, transportation construction will destroy the permafrost environment that has existed for many years. For example, the heat absorption of asphalt on the road and the exhaust emissions of vehicles along the corridor will increase the surface temperature of the area, thereby accelerating the melting of permafrost [1–3]. On the other hand, it will damage the surface vegetation and topsoil, accelerating soil erosion [4]. Due to the limited carrying capacity of resources and the environment in the Xizang region, it is difficult to restore the ecological environment once it is damaged [5]. Therefore, coordinating the construction of transportation infrastructure with the quality protection of the local ecological environment is a necessary path for the development of the Xizang region's economy. Timely evaluation of changes in the quality of the ecological environment in the area where linear engineering is located can help improve the negative impact of human activities on the environment [6].

In 2006, the Chinese Ministry of Environmental Protection proposed the ecological environment index (EI) for ecological environment assessment, but this index also has many issues in its application process, such as subjective weighting and lack of visualizable evaluation results [7]. Remote sensing technology has become an indispensable means of ecological monitoring and assessment [8]. Taking advantage of the spatial and temporal coverage of satellite data, Xu H Q [7] proposed an improved method called the remote sensing ecological index (RSEI) [7] based on the EI index. The evaluation indicators in this method mainly come from remote sensing indices. This method has been widely used in ecological environmental quality assessment research and has a high level of credibility [9–11]. For example, RSEI [7] has been applied in the evaluation of the surface water ecological environment in Freetown [11], the assessment of ecological environmental quality in the Samara region of Russia [12], and the evaluation of ecological conditions during the rainy and dry seasons in Kota Semarang [13]. In addition, researchers have also improved the evaluation algorithms and indicators based on the RSEI [7] from different perspectives. In terms of algorithm models, the RSEI initially mainly used the first principal component (PC1) of the principal component analysis (PCA) to construct the ecological index. However, the variance contribution rate of PC1 extracted in different studies varies greatly, which cannot guarantee a high contribution rate. In other words, the interpretation of the evaluation indicators obtained after dimensionality reduction is more unstable compared to the original indicators. Therefore, some scholars have made improvements to the model, such as using a modified remote sensing ecological index (MRSEI) to evaluate the ecological environment of the Xilingol League Grassland in China [14]. Machine learning has also been introduced, and the RSEI [7] time series data for Beijing, China, has been calculated using PCA combined with the random forest algorithm [15]. In terms of indicator systems, Karimi [16] used the land surface ecological status composition index (LESCI) based on the vegetation-impervious-soil triangle model to assess the surface ecological conditions in Iran, as well as some cities in Europe and North America [16]. Xing et al. used net primary productivity, vegetation index, and light index to construct an enhanced remote sensing ecological index for an ecological environment assessment of Hainan Island, China, based on local characteristics [17].

Determining appropriate indicator weights is essential in ecological environmental quality assessment. There are two types of weight determination methods: objective weight determination methods (OW) based on data mining and statistics [18], including entropy weight method (EWM) [19], random forest (RF) [20], and support vector machine (SVM) [21], and subjective weight determination methods (SW) based on prior knowledge or expert opinions, including analytic hierarchy process (AHP) [22], multi-criteria decision analysis (MCDM) [23], and fuzzy mathematics (FM) [24], among others. The subjective

weight method is influenced by prior knowledge, leading to higher subjectivity in the final evaluation results, while using only PCA for each indicator's weight assignment is too objective and may cause biased results due to the large amount of information [25]. Game theory (GT) is a mathematical model of strategic interaction between rational and irrational agents, which can effectively use SW and OW weight information to obtain combined weights (CW) [26]. Therefore, this study uses game theory (GT) to calculate weights, with PCA used as the objective weight assignment method and AHP as the subjective weight assignment method, to obtain optimal weights by balancing subjective and objective weights.

The Lhasa–Nyingchi Motorway from Nyingchi to Gongbo'gyamda section was put into use in September 2015, meeting the requirements for ecological environment assessment of highways (generally 3 to 5 years after completion and acceptance). Therefore, this study takes the Lhasa–Nyingchi Motorway from Nyingchi to Gongbo'gyamda section as an example, using a modified remote sensing ecological index to evaluate the ecological environmental quality within a 5 km range on both sides of the highway from 2012 to 2020, studying its change trends and analyzing the reasons for the change in order to provide reference and basis for the ecological environment restoration work after highway construction in the Xizang region.

## 2. Study Area and Materials

### 2.1. Study Area

The Lhasa–Nyingchi Motorway, also known as the Lhoka–Lhasa Expressway, has a total length of 409.2 km and is the first phase project of the "12th Five-Year Plan" key project in the Xizang region of China. The Nyingchi to Gongbo'gyamda section of the highway is 114.3 km long and runs parallel to the Lhasa to Nyingchi section of National Highway 318. It is primarily designed as a dual-carriageway with four lanes, and construction began in late May 2013. The section was officially opened to traffic on 15 September 2015. This section is located in the southeastern part of the Xizang region, in the northwest of Nyingchi Prefecture, with coordinates ranging from 29°31′N to 29°54′N and 93°10′E to 94°27′E. It is situated in the central part of Bayi District and the southeastern part of Gongbo'gyamda (Figure 1). Vegetation is the main component of the ecosystem in this region. The Nyang River valley area is mostly wetlands and water bodies, while the land use types around the highways are mainly forests and shrubs. Influenced by the warm and humid air currents of the Indian Ocean, the vegetation in the study area belongs to the semi-humid temperate mountain vegetation and has a clear vertical distribution pattern. The land use of the residential area is mainly farmland, with no obvious impervious areas. The region has a large range of elevation, a complex and diverse climate, and significant local climate differences, making it prone to natural disasters such as hailstorms, drought, or floods [27–30]. The highways mainly traverse the middle and lower reaches of the Nyang River valley, which is characterized by a wide valley landform with flat terrain, facilitating the implementation of linear engineering. However, there are risks of collapse and debris flows on the mountainsides on both sides of the Nyang River valley [31].
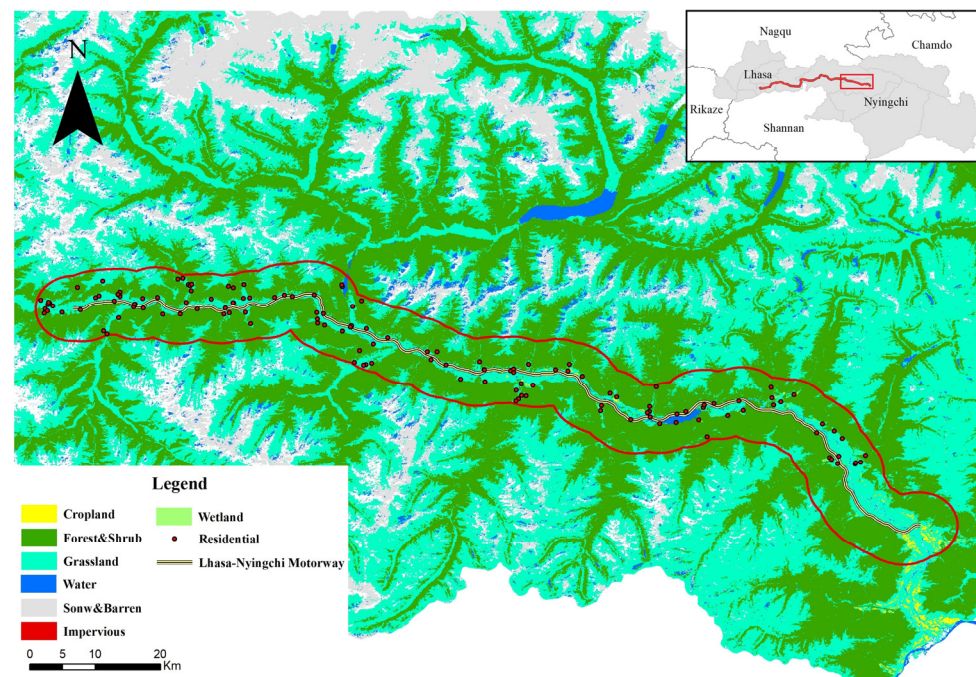
**Figure 1.** Location of Nyingchi to Gongbo'gyamda section of Lhasa–Nyingchi Motorway.

## 2.2. Data Source and Preprocessing

The remote sensing data used in this study mainly come from the MODIS (moderate-resolution imaging spectroradiometer) data provided by the Google Earth Engine (GEE) platform. MODIS is a remote sensing product carried by the Terra and Aqua satellites; it is used to observe global climate change and biological activities. The MODIS data products used in this study are processed and analyzed synthetic images, with imaging time ranging from July to September between 2012 and 2020. This period represents the peak growing season for vegetation in the Xizang region and helps distinguish vegetation areas from bare land and snow-covered areas. Five types of MODIS data products (Table 1) were used in this study. These data products have high quality and have undergone radiometric and atmospheric corrections. However, due to geometric distortions, geometric correction was performed using the reproject and resample functions in the GEE platform. Other data processing tasks, such as mosaicking, mask extraction, and uniform resolution, were also implemented by coding in the GEE platform. Finally, the indicator data for the study area could be calculated.

**Table 1.** Data details.

| Index | Product | Spatial Resolution (m) | Time Resolution (d) | Time |
|---|---|---|---|---|
| NDVI/FVC | MOD13Q1 | 250 | 16 | 2012–2020 |
| LAI | MCD15A3H | 500 | 8 | 2012–2020 |
| GPP | MOD17A2H | 500 | 8 | 2012–2020 |
| LST | MOD11A2 | 1000 | 8 | 2012–2020 |
| Wet | MOD09A1 | 500 | 8 | 2012–2020 |

## 2.3. Method

In recent years, vegetation changes have dominated ecological research in the Xizang region of China. The original RSEI (remote sensing ecological index) [6] only used vegetation indices (VI) to represent vegetation. However, in this study, considering the extremely limited ecological carrying capacity and increased sensitivity to greenhouse effects in the Qinghai-Xizang Plateau, detecting short-term vegetation changes becomes particularly important [32,33]. Therefore, this study incorporates the leaf area index (LAI), which re-

flects vegetation growth quality, and the gross primary productivity (GPP) index, which reflects vegetation carbon sequestration capacity, to improve the vegetation index in the evaluation system. Soil wetness can be used as an important indicator for monitoring soil degradation. Additionally, Yijin Wu [34] found that the land surface temperature (LST) in the Xizang region is positively correlated with vegetation growth; specifically, this abnormal phenomenon is manifested as follows: the larger the aridity index, the better the ecological environment. Therefore, this study uses the LST and the wetness (Wet) to replace the original TVDI(Temperature Vegetation Dryness Index). Finally, the five indicators of greenness (FVC, LAI, and GPP), warmth (LST), and wetness (Wet) were used to construct an improved RSEI [7] (MRSEI).

### 2.3.1. Indicator Calculation

(1)    Greenness

$FVC$ (Fractional Vegetation Cover) is the percentage of the area covered by vegetation in relation to the total surface area. It is a simple measure of vegetation coverage and growth and a key factor in soil and water conservation and ecological assessment [35]. $FVC$ can be used to estimate shrub biomass in high mountain or subalpine environments [36]. In this study, $FVC$ is derived using the normalized difference vegetation index ($NDVI$) and pixel-based binary method [37]. The $NDVI$ is primarily derived from MODIS data products, as shown in the following formula:

$$NDVI = NDVI_{veg} \times FVC + NDVI_{soil} \times (1 - FVC) \tag{1}$$

$NDVI_{veg}$ and $NDVI_{soil}$ represent the $NDVI$ values in areas with complete vegetation coverage and areas with complete bare soil or no vegetation coverage, respectively. The calculation formulas are as follows:

$$NDVI_{soil} = \frac{FVC_{max} \times NDVI_{min} - FVC_{min} \times NDVI_{max}}{FVC_{max} - FVC_{min}} \tag{2}$$

$$NDVI_{veg} = \frac{(1 - FVC_{min}) \times NDVI_{max} - (1 - FVC_{max}) \times NDVI_{min}}{FVC_{max} - FVC_{min}} \tag{3}$$

Since the MODIS data used in this study were acquired from July to September, which is the period of the year with the best vegetation growth in the study area, we can approximate that $FVC_{max}$ = 100% and $FVC_{min}$ = 0%. Based on the pixel-based binary method, the vegetation coverage model is defined as follows:

$$FVC = \frac{NDVI - NDVI_{min}}{NDVI_{max} - NDVI_{min}} \tag{4}$$

In the equation, $NDVI_{max}$ represents the normalized difference vegetation index value of pixels with vegetation coverage, while $NDVI_{min}$ represents the normalized difference vegetation index value of pixels with complete bare soil. Since the study area is mostly inaccessible and obtaining extensive field measurements is challenging, this study uses the confidence interval values of the cumulative frequency of $NDVI$ at 5% and 95% as the $NDVI_{min}$ and $NDVI_{max}$ values.

The leaf area index ($LAI$) is a dimensionless parameter that measures the amount of foliage in the canopy and is used to reflect the vegetation growth quality in the study area [38]. In this study, the MODIS data product MOD15A3H is used to obtain $LAI$ data for the study area. The calculation formula is as follows [39]:

$$LAI = 0.1 \times DN_A \tag{5}$$

$DN_A$ represents the gray value of the leaf area index image except for bare land, glaciers, or water areas.

Gross primary productivity (GPP) refers to the total amount of organic carbon fixed by vegetation through photosynthesis in a unit of time. The accumulation of organic carbon by vegetation is a driving force for multiple ecosystems and a key component of land carbon balance, mainly reflecting the carbon source-sink status of vegetation in the study area [40]. In this study, the MOD17A2H product of GPP is extracted at the grid level and dimensionless processing is applied to obtain the distribution of GPP in the study area.

(2)　Heat

The thermal index utilizes land surface temperature ($LST$), which refers to the surface temperature of the Earth's land surface that has been corrected for emissivity. It is measured in degrees Celsius (°C) and is an important surface parameter that controls the energy balance between the atmosphere and the land surface. The process of extracting $LST$ involves converting the digital number ($DN$) values from the MOD11A2 product data into Celsius to represent the distribution of land surface temperature in the study area. The calculation formula is as follows:

$$LST = 0.02 \times DN_S - 273.15 \tag{6}$$

(3)　Wet

This study utilizes a modified tasseled cap transformation (Kauth–Thomas, K–T) formula [41] to extract the wetness index. The K–T transformation is a method based on image physical characteristics, which uses a linear orthogonal transformation to project and transform multi-spectral remote sensing images into three-dimensional space. This method is used to reflect the degree of plant growth and withering, as well as changes in land information.

We use the MOD09A1 surface reflectance product, which is sensitive to land moisture information in certain bands, to calculate the humidity of the study area. The formula is as follows:

$$Wet = 0.1147\rho_1 + 0.2489\rho_2 + 0.2408\rho_3 + 0.3132\rho_4 - 0.3122\rho_5 - 0.6416\rho_6 - 0.5087\rho_7 \tag{7}$$

$\rho_1 \sim \rho_7$ The seven bands of reflectance in the MOD09A1 surface reflectance product are red, NIR1, Blue, Green, NIR2, SWIR1, and SWIR2.

2.3.2. Weight Determination

(1)　Principal component analysis (PCA)

Principal component analysis (PCA) is a commonly used statistical analysis method that can combine several correlated indicators into a mutually independent composite index through a linear transformation. The advantage of PCA is that it can reduce the dimensionality of the indicators while retaining the maximum principal components, and the determination of weights is objective. The steps for determining weights based on PCA are as follows: ① Standardize the original data. ② Calculate the correlation coefficient matrix of each indicator. ③ Calculate the eigenvalues, contribution rates, and cumulative contribution rates of each principal component. ④ Calculate the loading values of each principal component. ⑤ Obtain the scores of each principal component. ⑥ Calculate the weight of each indicator; the formula is as follows:

$$PC = \sum_{i=1}^{i} \frac{pc_i \times e_i}{\sqrt{k_i} \times E} \tag{8}$$

where $PC$ represents the score coefficient of each indicator, $pc_i$ represents the load of each principal component, $e_i$ represents the variance contribution rate of each principal component, $k_i$ represents the eigenvalues of each principal component, and $E$ represents the cumulative contribution rate of the extracted principal components. Finally, the weights of each indicator can be obtained by normalizing the $PC$.

(2)   Combination weight method based on game theory

Game theory (GT) can effectively utilize the combined information of subjective weights (SW) and objective weights (OW) and obtain the most balanced weights, also known as combined weights (CW). Supposing that the weight set generated by using a weighting method for m basic indicator vectors is $\omega_1$, the weight vector obtained by n empowerment methods is then $\omega_i$:

$$\omega_1 = [\omega_{11}, \omega_{12}, \omega_{13}, \ldots, \omega_{1m}] \tag{9}$$

$$\omega_i = [\omega_{n1}, \omega_{n2}, \omega_{n3}, \ldots, \omega_{nm}] = [\omega_1, \omega_2, \omega_3, \ldots, \omega_n], i = 1, 2, \ldots, n \tag{10}$$

The arbitrary linear combination *W* of the *n* vectors is as follows:

$$W = \sum_{i=1}^{n} \gamma_i \omega_i^T, \ i = 1, 2, \ldots, n \tag{11}$$

Solving the optimal combination coefficient $\gamma_i$ to minimize the deviation between the combination weight and the weight involved in optimization can be achieved through the following function:

$$\min || \sum_{i=1}^{n} \gamma_i \omega_i^T - \omega_i^T ||, i = 1, 2, \ldots, n \tag{12}$$

Solving the first derivative of the above equation for optimization yields the following equivalent linear equations:

$$\sum_{i=n}^{n} \gamma_i \omega_i \omega_i^T = \begin{bmatrix} \gamma_1 \\ \gamma_2 \\ \cdot \\ \cdot \\ \cdot \\ \gamma_n \end{bmatrix} \times \begin{bmatrix} \omega_1 \times \omega_1^T & \omega_1 \times \omega_2^T & \ldots & \omega_1 \times \omega_n^T \\ \omega_2 \times \omega_1^T & \omega_2 \times \omega_2^T & \ldots & \omega_2 \times \omega_n^T \\ \cdot & \cdot & \cdot & \cdot \\ \cdot & \cdot & \cdot & \cdot \\ \cdot & \cdot & \cdot & \cdot \\ \omega_n \times \omega_1^T & \omega_n \times \omega_2^T & \ldots & \omega_n \times \omega_n^T \end{bmatrix} = \begin{bmatrix} \omega_1 \times \omega_n^T \\ \omega_2 \times \omega_2^T \\ \cdot \\ \cdot \\ \cdot \\ \omega_n \times \omega_n^T \end{bmatrix} \tag{13}$$

The process of calculating the combined weight ($\gamma_1, \gamma_2, \ldots, \gamma_n$), and then standardizing it to obtain the optimal combination weight $\omega^*$, can be expressed as follows:

$$\omega^* = \sum_{i=1}^{n} \gamma_i \times \omega_i^T, i = 1, 2, \ldots, n \tag{14}$$

Finally, we use the comprehensive index method to calculate the comprehensive value of the ecological environment, the *MRSEI*, which can be expressed by the following formula:

$$MRSEI = \sum_{i=1}^{P} \omega_i^* * x_i \tag{15}$$

where $x_i$ represents the standardized value of the i-th indicator, $\omega_i^*$ represents the optimal combined weight of the i-th indicator, and *P* represents the number of evaluation indicators.

### 3. Results and Analysis

*3.1. PCA and Combination Weights*

This study utilized IBM SPSS Statistics 25.0 to perform a principal component analysis on the indicator data. Table 2 presents the results of the principal component analysis for the years 2012 and 2020. It can be observed that the cumulative contribution rates of the first three principal components are all greater than 85%, indicating that these three components capture the majority of the characteristics of the five indicators. Specifically, PC1 has high loading values for FVC, LAI, and GPP, PC2 has a high loading value for Wet, and PC3 has a high loading value for LST. Therefore, we can summarize the extracted

principal components as follows: PC1 represents the vegetation factor, represented by FVC, LAI, and GPP; PC2 represents the humidity factor, represented by Wet; and PC3 represents the thermal factor, represented by LST.

**Table 2.** Results of PCA in 2012 and 2020.

| Index | 2012 | | | 2020 | | |
|---|---|---|---|---|---|---|
| | PC1 | PC2 | PC3 | PC1 | PC2 | PC3 |
| FVC | 0.847 | −0.201 | −0.066 | 0.858 | −0.241 | 0.056 |
| LAI | 0.909 | −0.005 | −0.002 | 0.894 | −0.134 | −0.128 |
| GPP | 0.86 | −0.095 | 0.25 | 0.882 | −0.103 | −0.24 |
| Wet | 0.081 | 0.806 | 0.572 | 0.226 | 0.88 | −0.404 |
| LST | 0.293 | 0.65 | −0.693 | 0.496 | 0.439 | 0.745 |
| Eigenvalues | 2.375 | 1.123 | 0.874 | 2.61 | 1.053 | 0.794 |
| Variance Contribution Rate (%) | 47.5 | 22.454 | 17.479 | 52.201 | 21.059 | 15.884 |
| Total Contribution Rate (%) | 47.5 | 69.954 | 87.433 | 52.201 | 73.26 | 89.144 |

Based on the principal component analysis results, the weights for each indicator can be calculated for each year from 2012 to 2020. These weights are then combined with the weights obtained from the analytic hierarchy process (AHP) to calculate the composite weight coefficients. Taking 2012 and 2020 as examples, the final weights are shown in Table 3.

**Table 3.** Index weight in 2012 and 2020.

| Index | 2012 | | | 2020 | | |
|---|---|---|---|---|---|---|
| | OW | SW | CW | OW | SW | CW |
| FVC | 0.1750 | 0.3178 | 0.2412 | 0.1884 | 0.3178 | 0.2575 |
| LAI | 0.2367 | 0.1761 | 0.2086 | 0.1890 | 0.1761 | 0.1821 |
| GPP | 0.2477 | 0.1761 | 0.2145 | 0.1752 | 0.1761 | 0.1757 |
| Wet | 0.2570 | 0.165 | 0.2143 | 0.1439 | 0.165 | 0.1552 |
| LST | 0.0836 | 0.165 | 0.1214 | 0.3036 | 0.165 | 0.2295 |

*3.2. Analysis on the Overall Change Trend of Ecological Quality*

As shown in Table 4, the MRSEI values for the Lhasa–Nyingchi Motorway segment from Nyingch to Gongbo'gyamda in the years 2012–2020 are as follows: 0.5885, 0.5951, 0.5296, 0.6202, 0.59, 0.5777, 0.5898, 0.5703, and 0.5987. Overall, compared to before the construction of the highway in 2012, the MRSEI value in 2020 has slightly increased, but there is significant fluctuation in the MRSEI values each year. The MRSEI values showed a noticeable decrease from 2013 to 2014, which is closely related to highway construction. The MRSEI values then increased significantly from 2014 to 2015, mainly due to the implementation of ecological restoration projects. From 2015 to 2017, there was a slow decline in the MRSEI values, but from 2017 to 2020, the MRSEI values showed a stair-step growth trend, indicating that the ecological restoration work was challenging but that the ecological environmental quality was improving overall.

**Table 4.** MRSEI from 2012 to 2020.

| | 2012 | 2013 | 2014 | 2015 | 2016 | 2017 | 2018 | 2019 | 2019 |
|---|---|---|---|---|---|---|---|---|---|
| MRSEI | 0.5885 | 0.5951 | 0.5296 | 0.6202 | 0.59 | 0.5777 | 0.5898 | 0.5703 | 0.5987 |

Figure 2 shows the spatiotemporal changes in the ecological environmental quality of the study area. The MRSEI values were divided into five categories: poor, fair, moderate,

good, and excellent, with intervals of 0.2. It can be observed that in 2015, the ecological environmental quality was rated as good, while the rest of the years were rated as moderate. In terms of the spatial distribution of the MRSEI values in the nine periods, the ecological environmental quality gradually decreased from the eastern segment to the western segment. The areas with good and excellent ecological quality were mainly located in the southeastern part of the study area, where the humidity and temperature conditions were favorable and the vegetation coverage was relatively high. The areas with poor, fair, and moderate ecological quality were primarily located in the road area and the peripheral areas of the central and western segments. This is mainly due to the higher altitude and colder, drier climate in these areas, resulting in relatively lower vegetation coverage. The relatively poor ecological environmental quality in the western segment may also be related to the denser distribution of local residential areas.
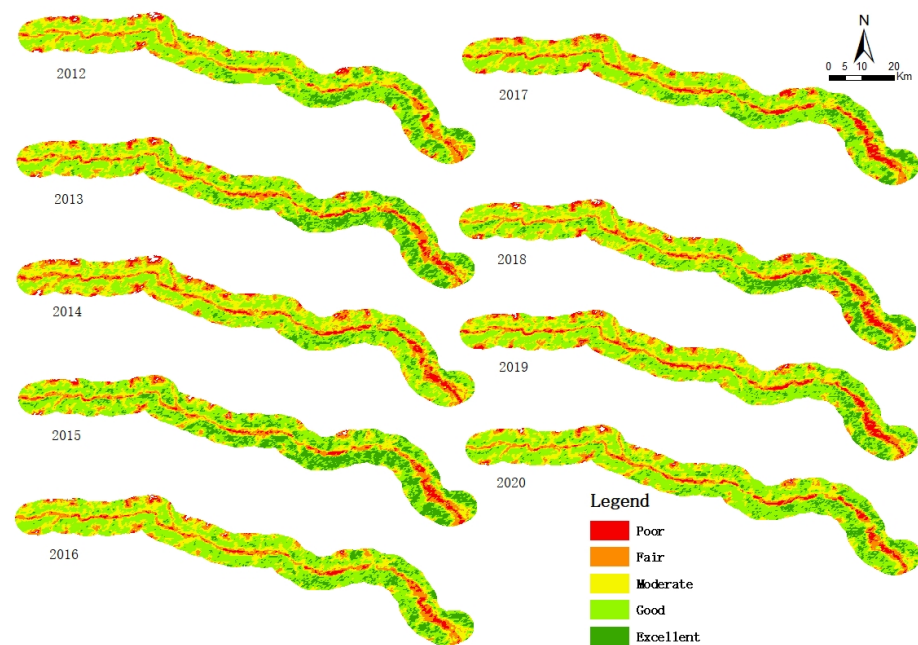


**Figure 2.** Spatial distribution of MRSEI values of the Nyingchi–Gongbo'gyamda section of the Lhasa–Nyingchi Motorway from 2012 to 2020.

The area and proportion of the ecological environmental quality in the study area for the nine periods were statistically analyzed (Table 5, Figure 3). It can be observed that the proportion of good ecological environmental quality was the largest, followed by the moderate category, from 2012 to 2020. The ecological environmental quality structure in 2012–2013 was similar, with the most significant variation occurring in 2014; the proportions of poor, fair, and moderate ecological quality were the highest in the nine-year period, and the MRSEI value was the lowest. Although the MRSEI value in 2015 was the highest in the nine years, there was no significant change in the area of good ecological quality compared to the previous year, and the area of moderate quality was the lowest in the nine years, decreasing by 9.72% compared to 2014. It is worth noting that in 2015, the area of excellent ecological quality reached 21.48%, which was nearly 10% higher than the average proportion of excellent quality in the other seven years, excluding 2014. This can be attributed to the construction period of the highway from 2013 to 2015, with full construction taking place in 2014, stripping the original vegetation and damaging the ecological environment along the route, resulting in a sudden decrease in the MRSEI value in 2014. However, in 2015, thanks to the smooth implementation of the highway ecological environment project, the MRSEI value rapidly increased. After the construction was completed, the construction facilities were removed, construction waste was cleared, depressions were leveled, and the original vegetation and turf were replanted, leading to a

significant improvement in the overall ecological environmental quality in a short period of time. Clearly, the ecological environmental quality in the road area and the peripheral areas of the study area has been significantly improved. The proportions of excellent, good, and moderate levels showed a declining trend in 2016 and 2017, indicating a slight rebound in the ecological restoration effect, mainly due to the higher requirements for transplanting vegetation in the high-altitude ecological environment. The ecological environmental quality structure in 2018 was similar to that in 2017, with similar proportions of excellent and good levels, but there was a noticeable increase in the proportion of excellent quality areas in 2018. Looking at Figure 2, it can be further observed that these increased areas were mainly located in the southern part of the eastern segment of the study area. Compared to 2018, the MRSEI value decreased in 2019, and the area of excellent quality decreased by 6.12%. Although there was a slight increase in the proportion of good-quality areas, the combined proportion of excellent and good levels was lower than in 2018. In 2020, the overall ecological quality level was good, with a 1.01% decrease in the area of excellent quality compared to 2012, while the area of good quality increased by 5.46% and had the highest proportion in the nine years. The area of moderate quality decreased by 2.74%, and the combined area of poor and fair levels was the smallest in the nine years. In conclusion, the ecological environmental quality in the study area in 2020 did not show significant changes compared to before the construction of the highway.

**Table 5.** Statistics of MRSEI area proportions in different years.

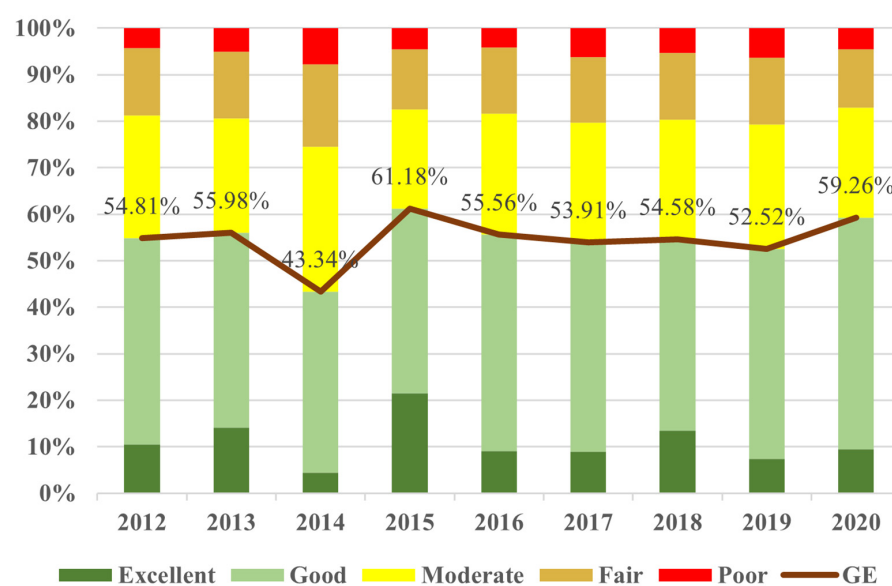|  | Excellent | | Good | | Moderate | | Fair | | Poor | |
|---|---|---|---|---|---|---|---|---|---|---|
|  | S/km$^2$ | Pct./% | S/km$^2$ | Pct./% | S/km$^2$ | Pct./% | S/km$^2$ | Pct./% | S/km$^2$ | Pct./% |
| 2012 | 172.8125 | 10.51 | 728.3125 | 44.3 | 434.4375 | 26.43 | 237.75 | 14.46 | 70.6875 | 4.3 |
| 2013 | 232.0625 | 14.12 | 688.25 | 41.86 | 405.0625 | 24.64 | 235.75 | 14.34 | 82.875 | 5.04 |
| 2014 | 72.5 | 4.41 | 640.0625 | 38.93 | 511.3125 | 31.1 | 292.6875 | 17.8 | 127.4375 | 7.75 |
| 2015 | 353.1875 | 21.48 | 652.6875 | 39.7 | 351.4375 | 21.38 | 211.5 | 12.86 | 75.1875 | 4.57 |
| 2016 | 147.8125 | 8.99 | 765.6875 | 46.57 | 428.5 | 26.06 | 234.125 | 14.24 | 67.875 | 4.13 |
| 2017 | 146.0625 | 8.88 | 740.3125 | 45.03 | 423.5 | 25.76 | 230.5 | 14.02 | 103.625 | 6.3 |
| 2018 | 221.125 | 13.45 | 676.1875 | 41.13 | 424.0625 | 25.79 | 234.75 | 14.28 | 87.875 | 5.35 |
| 2019 | 120.5 | 7.33 | 742.875 | 45.19 | 439.125 | 26.71 | 237.75 | 14.46 | 103.75 | 6.31 |
| 2020 | 156.1875 | 9.5 | 818.0625 | 49.76 | 389.4375 | 23.69 | 204.5 | 12.44 | 75.8125 | 4.61 |



**Figure 3.** Changes in the proportion of MRSEI levels in the Nyingchi–Gongbo'gyamda section of the Lhasa–Nyingchi Motorway from 2012 to 2020.

Furthermore, the sums of the proportions of good and excellent quality (GE%) were separately calculated. The GE% for the years 2012–2020 are as follows: 54.81%, 55.98%, 43.34%, 61.18%, 55.56%, 53.91%, 54.58%, 52.52%, and 59.26%. Obviously, the GE% initially decreased due to road construction, then increased due to the implementation of ecological environment projects and ecological restoration, followed by a stepwise increase.

*3.3. Analysis of the Spatial and Temporal Evolution of Ecological Quality*

In order to further analyze the dynamic changes in the ecological environmental quality of the Nyingchi–Gongbo'gyamda section from 2012 to 2020, Table 6 presents the calculation of the difference in the modified remote sensing ecological index (MRSEI) for every two years. The difference values are categorized into five levels: significantly deteriorated (−2), deteriorated (−1), essentially unchanged (0), improved (+1), and significantly improved (+2). Figure 4 provides a visual representation of the proportions of each category and their changes over time.

**Table 6.** Monitoring of the level of MRSEI changes from 2012 to 2020.

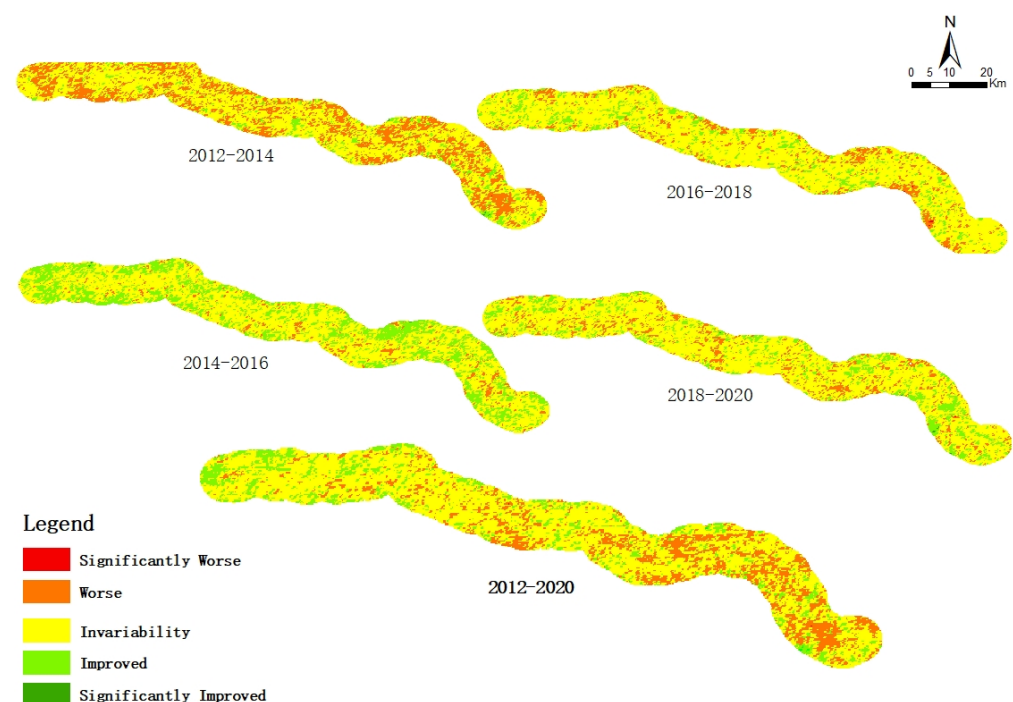| Years | The Ratio and Area of Changes | Significantly Worse | Worse | Invariability | Improved | Significantly Improved |
|---|---|---|---|---|---|---|
| 2012–2014 | Change Area (km²) | 0.3125 | 545.375 | 990.0625 | 107.4375 | 0.8125 |
| | Percentage (%) | 0.02 | 33.17 | 60.22 | 6.54 | 0.05 |
| 2014–2016 | Change Area (km²) | 0 | 86.0625 | 1028.125 | 529.1875 | 0.625 |
| | Percentage (%) | 0 | 5.23 | 62.54 | 32.19 | 0.04 |
| 2016–2018 | Change Area (km²) | 1.125 | 199.25 | 1243.75 | 199.875 | 0 |
| | Percentage (%) | 0.07 | 12.12 | 75.65 | 12.16 | 0 |
| 2018–2020 | Change Area (km²) | 0.4375 | 193.0625 | 1192.875 | 256.75 | 0.875 |
| | Percentage (%) | 0.03 | 11.74 | 72.56 | 15.62 | 0.05 |



**Figure 4.** Dynamic changes of the MRSEI in the Nyingchi–Gongbo'gyamda section of the Lhasa–Nyingchi Motorway from 2012 to 2020.

Combining Table 7 and Figure 5, it can be observed that the ecological quality remained relatively stable across the four periods. The proportion of areas with deteriorated ecological quality was highest in the 2012–2014 period, accounting for 33.17% of the total area. The proportions of areas with unchanged and improved ecological quality were the lowest in the four periods. Clearly, the construction of the highway had a significant impact on the local ecological environmental quality. Figure 4 reflects that the regions with deteriorated ecological environments were mainly located along the road and at the edges of the study area. During the 2014–2016 period, only 5.23% of the area experienced deteriorated MRSEI, while the proportion of areas with improved ecological quality reached 32.19%. This improvement can be attributed to the restoration effects of ecological environment projects. Overall, the ecological quality of the study area showed a positive trend. From the MRSEI changes in the 2016–2018 period, it can be seen that the ecological environmental quality in the study area exhibited a rebound trend. Looking at Figure 2, it is evident that the areas with deteriorated ecological quality were mainly located along the road and at the edges of the study area, indicating the high ecological sensitivity and the difficulty of ecological restoration in the alpine region. The changes in the 2018–2020 period were similar to the previous period. Looking at the 2016–2018 period, it can be observed that the proportion of areas with unchanged ecological quality tended to stabilize. With the continued efforts in ecological governance, the transplanted vegetation can better adapt to the local climate and environment.

**Table 7.** Monitoring of MRSEI changes in the Nyingchi–Gongbo'gyamda section of the Lhasa–Nyingchi Motorway from 2012 to 2020.

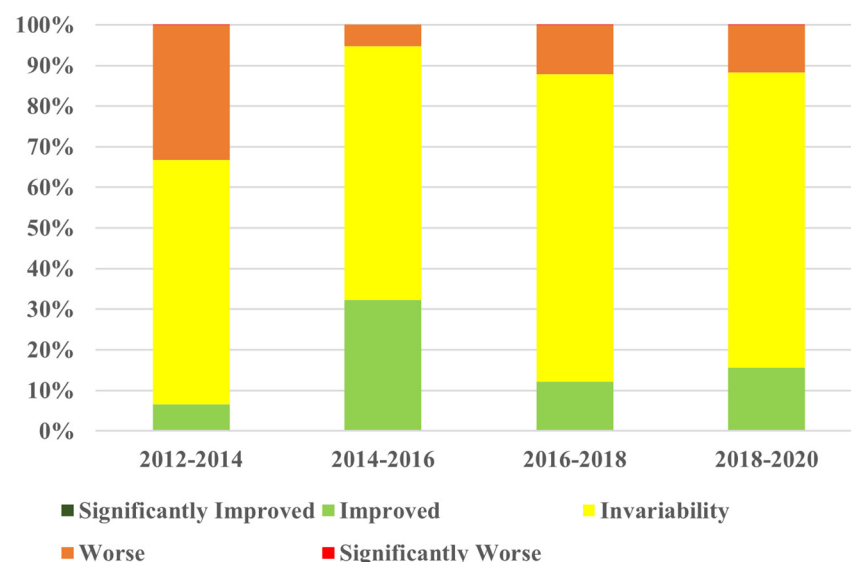| | Change Level | Change Area (km$^2$) | Percentage (%) | Total Change (km$^2$) | Total Percentage (%) |
|---|---|---|---|---|---|
| Improved | Significantly Improved | 1.9375 | 0.12 | 289 | 17.58 |
| | Improved | 287.0625 | 17.46 | | |
| Invariability | Invariability | 1142.5 | 69.5 | 1142.5 | 69.5 |
| Degenerate | Worse | 212.375 | 12.92 | 212.5 | 12.93 |
| | Significantly Worse | 0.1215 | 0.01 | | |



**Figure 5.** Changes in the level of the MRSEI from 2012 to 2020.

Table 7 presents the calculation of the MRSEI difference between the year before road construction in 2012 and the fifth year after road implementation in 2020. It is evident that the overall ecological quality in the study area remained relatively stable from 2012 to 2020, with a value of 69.5%. The majority of this ecological quality was concentrated

in the western and central parts of the study area. Additionally, a significant proportion (17.58%) of the area experienced improvement in ecological environmental quality, mainly located in the central and western sections, as well as the periphery of the entire study area. Lastly, there were areas where ecological quality degraded, primarily in the eastern-central part of the study area. Table 8 analyzes the overall changes in ecological quality using a transition matrix. With the exception of the "excellent" and "poor" levels, the proportion of each ecological quality level that remained unchanged was the largest. Additionally, the proportion of transitions between two or more levels was relatively small, regardless of whether the changes were "improved" or "degenerate". For each level, except for the "excellent" level, the proportion of improvements was greater than that of degradations.

**Table 8.** Level transfer matrix of the MRSEI for the Nyingchi–Gongbo'gyamda section of the Lhasa–Nyingchi Motorway from 2012 to 2020 (%).

| | | 2012 | | | | |
|---|---|---|---|---|---|---|
| | Level | Excellent | Good | Moderate | Fair | Poor |
| | Excellent | 33.35 | 12.88 | 0.95 | 0.21 | 0.18 |
| | Good | 65.39 | 75.98 | 32.10 | 4.57 | 1.95 |
| 2020 | Moderate | 1.27 | 10.36 | 54.22 | 29.60 | 8.31 |
| | Fair | 0.00 | 0.71 | 11.57 | 49.21 | 45.36 |
| | Poor | 0.00 | 0.07 | 1.17 | 16.40 | 44.21 |
| | Rate of change | 9.62 | −12.32 | 10.36 | 13.99 | −7.25 |

From the perspective of MRSEI level transitions, the proportions and areas of land that did not undergo transitions from the "excellent" to "poor" ecological quality levels are as follows: 33.35%/57.625 km$^2$, 75.98%/553.375 km$^2$, 54.22%/235.5625 km$^2$, 49.21%/117 km$^2$, and 44.21%/31.25 km$^2$. Among them, the land with "good" and "fair" ecological quality levels had a larger area that did not undergo any transitions. Therefore, the land with unchanged ecological environmental quality from 2012 to 2020 was mainly dominated by "good" and "fair" levels.

In terms of improvements in ecological environmental quality levels, the proportions and areas of land that transitioned from "poor", "fair", "moderate", and "good" to the next higher level are as follows: 45.36%/32.0625 km$^2$, 29.61%/70.375 km$^2$, 32.1%/139.4375 km$^2$, and 12.88%/93.8125 km$^2$, respectively. It is evident that there was a significant increase in the areas for all categories. Therefore, improvements in ecological environmental quality were evident in all four levels: "poor", "fair", "moderate", and "good". In terms of degradation types, the proportions and areas of land that transitioned from "excellent", "good", "moderate", and "fair" to the next lower level are as follows: 65.39%/113 km$^2$, 10.36%/75.4375 km$^2$, 11.57%/50.25 km$^2$, and 16.4%/39 km$^2$, respectively. It can be seen that there was a higher proportion of degradation in the "excellent" and "good" categories. Therefore, the degradation of ecological quality mainly occurred in the transition from "excellent" to "good" and "good" to "fair". In summary, the ecological environmental quality in the study area was slightly better in 2020 than in 2012, with more obvious improvements in the central and western sections. The areas with significant ecological degradation were mainly located in the eastern part of the study area, where the "excellent" and "good" ecological quality levels were degraded to "good" and "moderate", respectively.

## 4. Conclusions

This study mainly utilized MODIS data from the GEE platform and combined it with the characteristics of the Xizang region. By introducing a combination weighting method based on GT, the RSEI was improved to evaluate the ecological environmental quality of the Lhasa–Nyingchi Motorway's Nyingchi to Gongbo'gyamda section. The main conclusions are as follows:

(1)   The overall ecological environmental quality of the Nyingchi to Gongbo'gyamda section has significant regional differences. The quality of the ecological environment

decreases from east to west. In the central and eastern sections, the ecological environmental quality is better on the southern side compared to the northern side. The areas with better ecological quality are mainly located in the southeastern part, while areas with poor, fair, and moderate ecological quality are mainly located in the roadside areas and the peripheral regions of the central and western sections.

(2) During the process of highway construction and operation, the ecological environmental quality shows a trend of "initial decline, subsequent improvement, and then a stair-step increase". The construction of the highway is the primary driver of ecological degradation in the study area, significantly reducing its ecological environmental quality. However, short-term ecological restoration and compensation efforts have allowed for the recovery of the ecological environmental quality, followed by a stair-step growth. This is mainly due to the strong ecological sensitivity of the Xizang region, as well as its unique geographical and climatic characteristics such as high altitude and large diurnal temperature differences, which increase the difficulty of ecological restoration.

(3) The ecological environmental quality in the study area from 2012 to 2020 mainly remained unchanged; with the area of improved ecological quality being greater than the degraded area, the ecological restoration project of the Lhasa–Nyingchi Motorway has shown significant effectiveness. The unchanged rate of ecological environmental quality is 69.5%, mainly occurring in good and moderate levels. In the area where the quality of the ecological environment has changed, there were significant improvements in all four levels of ecological quality: poor, fair, moderate, and good, mainly occurring in the middle and western sections. The types of ecological quality degradation mainly transformed from excellent to good and good to moderate, with the transformation being more pronounced in the central and eastern parts of the study area.

Overall, the assessment results validate the importance of ecological restoration projects. However, it is worth noting that due to the high cloud cover in the Nyingchi region from July to September, both Landsat and Sentinel data were not available for use in this study. As a result, the assessment primarily relied on MODIS imagery data and lacked consideration of factors such as meteorology and economic development. In future research, the focus will be on integrating high-temporal-resolution land satellite data, meteorological data, and other relevant factors for a more in-depth analysis. This aims to further enhance the effectiveness of ecological restoration in the Xizang region.

**Author Contributions:** Methodology, P.J.; Data curation, J.Y. and S.S.; Writing—original draft, X.W.; Project administration, X.H.; Funding acquisition, Q.L. and Z.M. All authors have read and agreed to the published version of the manuscript.

**Data Availability Statement:** The data presented in this study are available on request from the corresponding author.

**Conflicts of Interest:** Author Pengfei Jia was employed by the company Citic Construction Co., Ltd. The remaining authors declare that the research was conducted in the absence of any commercial or financial relationships that could be construed as a potential conflict of interest.

## References

1.  Sheng, Y.; Cao, Y.B.; Li, J.; Wu, J.C.; Chen, J.; Feng, Z.L. Characteristics of permafrost along Highway G214 in the Eastern Qinghai-Tibet Plateau. *J. Mt. Sci.* **2015**, *12*, 1135–1144. [CrossRef]
2.  Wu, Q.; Li, X.; Li, W. The Prediction of Permafrost Change along Qinghai–Tibet Highway, China. *Permafr. Periglac. Process.* **2015**, *11*, 371–376.

3.   Jin, H.; Zhao, L.; Wang, S.; Jin, R. Thermal regimes and degradation modes of permafrost along the Qinghai-Tibet Highway. *Sci. China* **2006**, *49*, 1170–1183. [CrossRef]

4.   Lin, Z.J.; Niu, F.J.; Luo, J.; Lu, J.H.; Liu, H. Changes in permafrost environments caused by construction and maintenance of Qinghai-Tibet Highway. *J. Cent. South Univ. Technol.* **2011**, *18*, 1454–1464. [CrossRef]

5.   Yang, D.; Qiu, H.; Hu, S.; Pei, Y.; Wang, X.; Du, C.; Long, Y.; Cao, M. Influence of successive landslides on topographic changes revealed by multitemporal high-resolution UAS-based DEM. *Catena* **2021**, *202*, 105229. [CrossRef]

6.   Nip, M.J.; Haes, H. Ecosystem approaches to environmental quality assessment. *Environ. Manag.* **1995**, *19*, 135–145. [CrossRef]

7.   Xu, H.Q. A remote sensing index for assessment of regional ecological changes. *China Environ. Sci.* **2013**, *33*, 889–897.

8.   Wu, J.; Wang, X.; Zhong, B.; Yang, A.; Jue, K.; Wu, J.; Zhang, L.; Xu, W.; Wu, S.; Zhang, N.; et al. Ecological environment assessment for Greater Mekong Subregion based on Pressure-State-Response framework by remote sensing. *Ecol. Indic.* **2020**, *117*, 106521. [CrossRef]

9.   Shan, W.; Jin, X.; Ren, J.; Wang, Y.; Xu, Z.; Fan, Y.; Gu, Z.; Hong, C.; Lin, J.; Zhou, Y. Ecological environment quality assessment based on remote sensing data for land consolidation. *J. Clean. Prod.* **2019**, *239*, 118126. [CrossRef]

10.  Xiong, Y.; Xu, W.; Lu, N.; Huang, S.; Wu, C.; Wang, L.; Dai, F.; Kou, W. Assessment of spatial–temporal changes of ecological environment quality based on RSEI and GEE: A case study in Erhai Lake Basin, Yunnan province, China—ScienceDirect. *Ecol. Indic.* **2021**, *125*, 107518. [CrossRef]

11.  Kamara, D.M.; Yang, Z.; Alhaji, L.Y. Ecological Geospatial Monitoring and Assessment of Surface Water Environment Using Remote Sensing Ecological Index Model (RSEI) in Freetown, Sierra Leone, from 2010 to 2018. *Glob. Sci. J.* **2020**, *8*, 45978.

12.  Boori, M.S.; Choudhary, K.; Paringer, R.; Kupriyanov, A. Eco-environmental quality assessment based on pressure-state-response framework by remote sensing and GIS. *Remote Sens. Appl. Soc. Environ.* **2021**, *23*, 100530. [CrossRef]

13.  Indrawati, L.; Murti, B.; Rachmawati, R. Integrated ecological index (IEI) for urban ecological status based on remote sensing data: A study at Semarang—Indonesia. *IOP Conf. Ser. Earth Environ. Sci.* **2020**, *500*, 012074. [CrossRef]

14.  Song, M.J.; Luo, Y.Y.; Duan, L.M. Evaluation of Ecological Environment in the Xilin Gol Steppe Based on Modified Remote Sensing Ecological Index Model. *Arid Zone Res.* **2019**, *36*, 1521–1527.

15.  Gou, R.; Zhao, J. Eco-Environmental Quality Monitoring in Beijing, China, Using an RSEI-Based Approach Combined with Random Forest Algorithms. *IEEE Access* **2020**, *8*, 196657–196666. [CrossRef]

16.  Firozjaei, M.K.; Fathololoumi, S.; Kiavarz, M.; Biswas, A.; Homaee, M.; Alavipanah, S.K. Land Surface Ecological Status Composition Index (LSESCI): A novel remote sensing-based technique for modeling land surface ecological status. *Ecol. Indic.* **2021**, *123*, 107375. [CrossRef]

17.  Wang, X.; Liu, C.; Fu, Q.; Yin, B. Construction and Application of Enhanced Remote Sensing Ecological Index. *Int. Arch. Photogramm. Remote Sens. Spat. Inf. Sci.* **2018**, *42*, 1809–1813. [CrossRef]

18.  Lai, C.; Chen, X.; Wang, Z.; Yu, H.; Bai, X. Flood Risk Assessment and Regionalization from Past and Future Perspectives at Basin Scale. *Risk Anal.* **2020**, *40*, 1399–1417. [CrossRef]

19.  Huang, S.; Ming, B.; Huang, Q.; Leng, G.; Hou, B. A Case Study on a Combination NDVI Forecasting Model Based on the Entropy Weight Method. *Water Resour. Manag. Int. J. Publ. Eur. Water Resour. Assoc.* **2017**, *31*, 3667–3681. [CrossRef]

20.  Liaw, A.; Wiener, M. Classification and Regression by random Forest. *R News* **2002**, *23*, 18–22.

21.  Foody, G.M.; Mathur, A. Toward intelligent training of supervised image classifications: Directing training data acquisition for SVM classification. *Remote Sens. Environ.* **2004**, *93*, 107–117. [CrossRef]

22.  Orencio, P.M.; Fujii, M. A localized disaster-resilience index to assess coastal communities based on an analytic hierarchy process (AHP). *Int. J. Disaster Risk Reduct.* **2013**, *3*, 62–75. [CrossRef]

23.  Stewart, T.J. Multicriteria Decision Analysis. In *International Encyclopedia of Statistical Science*; Lovric, M., Lovric, M., Eds.; Springer: Berlin/Heidelberg, Germany, 2011; pp. 872–875.

24.  Bahar Gogani, M.; Douzbakhshan, M.; Shayesteh, K.; Ildoromi, A.R. New Formulation of Fuzzy Comprehensive Evaluation Model in Groundwater Resources Carrying Capacity Analysis. *Ecopersia* **2018**, *6*, 79–89.

25.  Zou, Q.; Liao, L.; Qin, H. Fast Comprehensive Flood Risk Assessment Based on Game Theory and Cloud Model Under Parallel Computation (P-GT-CM). *Water Resour. Manag.* **2020**, *34*, 1625–1648. [CrossRef]

26.  Wu, T.Y.; Lee, W.T.; Guizani, N.; Wang, T.M. Incentive mechanism for P2P file sharing based on social network and game theory. *J. Netw. Comput. Appl.* **2014**, *41*, 47–55. [CrossRef]

27.  Zhou, W.; Qiu, H.; Wang, L.; Pei, Y.; Tang, B.; Ma, S.; Yang, D.; Cao, M. Combining rainfall-induced shallow landslides and subsequent debris flows for hazard chain prediction. *Catena* **2022**, *213*, 106199. [CrossRef]

28.  Ma, S.; Qiu, H.; Yang, D.; Wang, J.; Zhu, Y.; Tang, B.; Sun, K.; Cao, M. Surface multi-hazard effect of underground coal mining. *Landslides* **2022**, *20*, 39–52. [CrossRef]

29.  Liu, Z.; Qiu, H.; Zhu, Y.; Liu, Y.; Yang, D.; Ma, S.; Zhang, J.; Wang, Y.; Wang, L.; Tang, B. Efficient Identification and Monitoring of Landslides by Time-Series InSAR Combining Single- and Multi-Look Phases. *Remote Sens.* **2022**, *14*, 1026. [CrossRef]

30.  Wang, L.; Qiu, H.; Zhou, W.; Zhu, Y.; Liu, Z.; Ma, S.; Yang, D.; Tang, B. The post-failure spatiotemporal deformation of certain translational landslides may follow the pre-failure pattern. *Remote Sens.* **2022**, *14*, 2333. [CrossRef]

31.  Li, T.; Sun, G.; Huang, J. Analysis on Typical Route Selection along River of High-grade Lhasa-Nyingchi Highway. *Urban Roads Bridges Flood Control* **2018**, *8*, 27–30+8.

32. Piao, S.L.; Fang, J.Y. Seasonal changes in vegetation activity in response to climate changes in China between 1982 and 1999. *Acta Geogr. Sin.* **2003**, *58*, 119–125.

33. Zhong, L.; Ma, Y.M.; Salama, M.S.; Su, B. Assessment of vegetation dynamics and their response to variations in precipitation and temperature in the Tibetan Plateau. *Clim. Chang.* **2010**, *103*, 519–535. [CrossRef]

34. Wu, Y.J.; Zhao, X.; Xi, Y.; Liu, H.; Li, C. Comprehensive evaluation and spatial-temporal changes of eco-environmental quality based on MODIS in Tibet during 2006–2016. *Acta Geogr. Sin.* **2019**, *74*, 1438–1449.

35. Bing, G.; Fang, H.; Lin, J. An Improved Dimidiated Pixel Model for Vegetation Fraction in the Yarlung Zangbo River Basin of Qinghai-Tibet Plateau. *J. Indian Soc. Remote Sens.* **2017**, *46*, 219–231.

36. Zhang, L.; Cui, G.; Shen, W.; Liu, X. Cover as a simple predictor of biomass for two shrubs in Tibet. *Ecol. Indic.* **2016**, *64*, 266–271. [CrossRef]

37. Leprieur, C.; Verstraete, M.; Pinty, B. Evaluation of the performance of various vegetation indices to retrieve vegetation cover from AVHRR data. *Remote Sens. Rev.* **1994**, *10*, 265–284. [CrossRef]

38. Asner, G.P.; Scurlock, J.; Hicke, J.A. Global synthesis of leaf area index observations: Implications for ecological and remote sensing studies. *Glob. Ecol. Biogeogr.* **2003**, *12*, 191–205. [CrossRef]

39. Jensen, J.L.; Humes, K.S.; Hudak, A.T.; Vierling, L.A.; Delmelle, E. Evaluation of the MODIS LAI product using independent lidar-derived LAI: A case study in mixed conifer forest. *Remote Sens. Environ.* **2011**, *115*, 3625–3639. [CrossRef]

40. Schaefer, K.; Schwalm, C.R.; Williams, C.; Arain, M.A.; Barr, A.; Chen, J.M.; Davis, K.J.; Dimitrov, D.; Hilton, T.W.; Hollinger, D.Y.; et al. A model-data comparison of gross primary productivity: Results from the North American Carbon Program Site Synthesis. *J. Geophys. Res. Biogeosci.* **2012**, *117*, G03010. [CrossRef]

41. Lobser, S.E.; Cohen, W.B. MODIS tasselled cap: Land cover characteristics expressed through transformed MODIS data. *Int. J Remote Sens.* **2007**, *28*, 5079–5101. [CrossRef]